Budker INP 2002-2
January 2002

Novosibirsk hadronic currents for $\tau \to 4\pi$ channels of τ decay library TAUOLA [†]

A. E. Bondar[a], S. I. Eidelman[a], A. I. Milstein[a], T. Pierzchała[b], N. I. Root[a], Z. Wąs[c,d] and M. Worek[b]

[a] *Budker Institute of Nuclear Physics*
Academician Lavrentyev 11, 630090 Novosibirsk-90, Russia
[b] *Institute of Physics, University of Silesia*
Uniwersytecka 4, 40-007, Katowice, Poland
[c] *Institute of Nuclear Physics*
Kawiory 26a, 30-055 Cracow, Poland
[d] *CERN, Theory Division, 1211 Geneva 23, Switzerland*

Abstract

The new parameterization of form factors developed for 4π channels of the τ lepton decay and based on Novosibirsk data on $e^+e^- \to 4\pi$ has been coded in a form suitable for the `TAUOLA` Monte Carlo package. Comparison with results from `TAUOLA` using another parameterization, *i.e.* the CLEO version of 1998 is also included.

To be submitted to Comput. Phys. Commun.

[†] Work supported in part by the Polish State Committee grants KBN 5P03B09320, 5P03B10721 and NATO Grant PST.CLG.977751, European Commission 5-th Framework contract HPRN-CT-2000-00149.

1 Introduction

Hadronic decays of the τ lepton offer a unique laboratory for studying hadronic interactions at low energies (below the τ lepton mass M). Proper modeling of such processes will facilitate comparison of experiment and theoretical models and may thus offer a crucial hint toward better understanding of low energy phenomenology of strong interactions. In this work we consider the τ decay into four pions and neutrino. Several models of this decay are at present in use [1–6]. While Refs. [1, 2] make an attempt to construct the Lagrangian of the decay from general theoretical principles, other models are purely phenomenological using either the experimental information from τ decays like in Refs. [3, 4] or from e^+e^- annihilation like in Refs. [5, 6]. In the following let us concentrate on the latter approach.

Production of four pions is one of the dominant processes of e^+e^- annihilation into hadrons in the energy range from 1.05 to 2.5 GeV. The hypothesis of the conserved vector current (CVC) relates to each other the cross section of this process and $\tau \to 4\pi\nu$ decay [7]. Therefore, all realistic models which describe the first process should also properly describe the other one. For a recent review of theoretical predictions for various decay modes of the τ based on CVC see *e.g.* [8].

For more than five years, two new detectors CMD-2 [9] and SND [10] have been studying low energy e^+e^- annihilation at the e^+e^- collider VEPP-2M at Novosibirsk. Their results can be used to provide a new parameterization of the form factors used in the Monte Carlo generators of the τ lepton. In the present paper we define the form factors which can be used as one of the possibilities in `TAUOLA` [11–13], the τ decay library. The `TAUOLA` package is organized in such a way that the phase space generation and calculation of the electroweak part of the matrix element are separated from the part of the code calculating the hadronic current provided by the particular model. This is convenient not only for constructing the Monte Carlo program, but also facilitates comparisons between different models. The technical description of the solution which allows an easy replacement of different hadronic currents is described in [14, 15].

Our paper is organized as follows: in the next section we recall basic principles of how e^+e^- data can be used in defining hadronic currents for the τ lepton decay. In Section 3 we describe those parts of the `TAUOLA` Monte Carlo algorithm for four pion generation and general formalism for the semileptonic/semihadronic decays which are needed for the definition of hadronic currents. In Section 4 we describe the new current for the 4π decay of the τ while in Section 5 details of the functions and constants used in this work are presented. Section 6 is devoted to technical tests of our code. Section 7 shows the comparison of numerical results from running the new version of `TAUOLA` with the relatively old one based on the CLEO parameterization [16–19] which is still widely in use despite the recent significant progress achieved by CLEO [3, 4]. Chapter 8 briefly summarizes the main results of the paper.

In Appendices we describe some technical aspects of our model. In particular, we tabulate the functions $G(Q^2)$ used for the definition of the hadronic current.

2 Relation between τ decays and e^+e^- annihilation cross sections

Via the hypothesis of conserved vector current one can relate the charged vector current coupling to the 4π system to the electromagnetic (neutral vector) current measured by $\sigma(e^+e^- \to \gamma \to 4\pi)$. There are two possible final states in e^+e^- annihilation [1]

$$\begin{aligned} e^+e^- &\to \gamma^* \to \tilde{\rho}^0 \to \pi^-\pi^-\pi^+\pi^+, \\ e^+e^- &\to \gamma^* \to \tilde{\rho}^0 \to \pi^+\pi^-\pi^0\pi^0, \end{aligned} \tag{1}$$

They are accessible by a different I_3 component of the same $I = 1$ weak current describing τ decay:

$$\begin{aligned} \tau^+ &\to W^+\bar{\nu}_\tau \to \tilde{\rho}^+\bar{\nu}_\tau \to \bar{\nu}_\tau\pi^+\pi^0\pi^0\pi^0, \\ \tau^+ &\to W^+\bar{\nu}_\tau \to \tilde{\rho}^+\bar{\nu}_\tau \to \bar{\nu}_\tau\pi^+\pi^-\pi^+\pi^0. \end{aligned} \tag{2}$$

The relations between processes (1) and (2) can be written as

$$\Gamma(\tilde{\rho}^+ \to \pi^+\pi^-\pi^+\pi^0) = \frac{1}{2}\Gamma(\tilde{\rho}^0 \to \pi^+\pi^-\pi^+\pi^-) + \Gamma(\tilde{\rho}^0 \to \pi^+\pi^-\pi^0\pi^0), \tag{3}$$

$$\Gamma(\tilde{\rho}^+ \to \pi^+\pi^0\pi^0\pi^0) = \frac{1}{2}\Gamma(\tilde{\rho}^0 \to \pi^+\pi^-\pi^+\pi^-). \tag{4}$$

The prediction for $\Gamma(\tau^+ \to \bar{\nu}_\tau X^+)$ can thus be obtained from $e^+e^- \to 4\pi$ data and isospin invariance. Such a procedure was successfully applied in [5] where high statistics e^+e^- data from the CMD-2 detector collected at center of mass energies (Q) from 1.05 to 1.38 GeV were used [6]. Since e^+e^- experiments are performed at fixed (at a time) Q, the integrated decay rates of $\tilde{\rho}^0$ to the 4π are well measured as a function of Q. Thus, the natural way of the τ decay generation is to generate first the mass of the 4π system in accordance with the experimental distribution. Then, for the fixed Q^2, the $\tilde{\rho}^0 \to 4\pi$ decay is generated. This is why in Ref. [5] the $d\Gamma/dQ^2$ distribution is generated independently of the differential distribution within the 4π system. The program is written and optimized to get maximum possible information from the experimental data.

The approach of `TAUOLA` is somewhat different. A matrix element well isolated in a program module is separated into the hadronic and leptonic current. All physical assumptions on hadronic interactions are located in the hadronic current which features intermediate state resonances as well as other properties of the hard process. The phase space density generation and in particular the appropriate jacobians for mapping random numbers to phase space coordinates, which are defined independently from the particular process, are also calculated in the separate part of the code. Such an approach provides flexibility in studying particular choices of hadronic currents. In addition, the Q^2 distribution is not an input, but originates from the (partial) Monte Carlo integration of the matrix element over phase space.

The aim of this paper is to use the model of [5] in the approach of `TAUOLA` which is more natural for comparison with other theoretical calculations/models.

[1] The $e^+e^- \to \pi^0\pi^0\pi^0\pi^0$ channel is forbidden by isospin and charge conjugation invariance.

3 General formalism for semileptonic decays

The matrix element used in TAUOLA for the semileptonic decay $\tau(P,s) \to \nu_\tau(N)X$ is written in the form:

$$\mathcal{M} = \frac{G}{\sqrt{2}}\bar{u}(N)\gamma^\mu(v+a\gamma_5)u(P)J_\mu \tag{5}$$

where $J_\mu \equiv < X|V_\mu - A_\mu|0 >$ denotes the matrix element of the $V-A$ current, relevant for the specific final state X. In general, the current J_μ depends on the momenta of all hadrons. N and P denote the four-momenta of the ν_τ and τ respectively. The squared matrix element for the decay of τ with mass M and spin s reads:

$$\begin{aligned}
|\mathcal{M}|^2 &= G^2\frac{v^2+a^2}{2}(\omega + H_\mu s^\mu),\\
\omega &= P^\mu(\Pi_\mu - \gamma_{va}\Pi^5_\mu),\\
H_\mu &= \frac{1}{M}(M^2\delta^\nu_\mu - P_\mu P^\nu)(\Pi^5_\nu - \gamma_{va}\Pi_\nu)
\end{aligned} \tag{6}$$

with

$$\begin{aligned}
\Pi_\mu &= 2[(J^*\cdot N)J_\mu + (J\cdot N)J^*_\mu - (J^*\cdot J)N_\mu],\\
\Pi^{5\mu} &= 2\ \mathrm{Im}\ \epsilon^{\mu\nu\rho\sigma}J^*_\nu J_\rho N_\sigma,\\
\gamma_{va} &= -\frac{2va}{v^2+a^2}
\end{aligned} \tag{7}$$

($\gamma_{va}=1$ in the Standard Model). If a more general coupling $v+a\gamma_5$ for the τ current and ν_τ mass $m_\nu \neq 0$ are expected to be used, one has to add the following terms to ω and H_μ:

$$\begin{aligned}
\hat{\omega} &= 2\frac{v^2-a^2}{v^2+a^2}m_\nu M(J^*\cdot J),\\
\hat{H}^\mu &= -2\frac{v^2-a^2}{v^2+a^2}m_\nu\ \mathrm{Im}\ \epsilon^{\mu\nu\rho\sigma}J^*_\nu J_\rho P_\sigma.
\end{aligned} \tag{8}$$

To obtain the polarimeter vector h in the τ rest frame, it is sufficient to calculate the space components of $h_\mu = (H_\mu + \hat{H}_\mu)/(\omega+\hat{\omega})$ and set $h_0 = 0$. The differential partial width for the channel under consideration reads:

$$d\Gamma_X = G^2\frac{v^2+a^2}{4M}d\mathrm{Lips}(P;q_i,N)(\omega+\hat{\omega}+(H_\mu+\hat{H}_\mu)s^\mu). \tag{9}$$

The phase space distribution for the final state with four mesons plus neutrino is given by the following expression where a compact notation with $q_5 = N$ and $q_i^2 = m_i^2$ is used,

$$d\mathrm{Lips}(P;q_1,q_2,q_3,q_4,q_5) = \frac{1}{2^{23}\pi^{11}}\ dQ^2\ dQ_3^2\ dQ_2^2 \qquad \times$$

$$d\Omega_5 \frac{\sqrt{\lambda(M^2,Q^2,m_5^2)}}{M^2} d\Omega_4 \frac{\sqrt{\lambda(Q^2,Q_3^2,m_4^2)}}{Q^2} d\Omega_3 \frac{\sqrt{\lambda(Q_3^2,Q_2^2,m_3^2)}}{Q_3^2} d\Omega_2 \frac{\sqrt{\lambda(Q_2^2,m_2^2,m_1^2)}}{Q_2^2} \quad (10)$$

where

$$Q^2 = (q_1+q_2+q_3+q_4)^2, \qquad Q_3^2 = (q_1+q_2+q_3)^2, \qquad Q_2^2 = (q_1+q_2)^2,$$

$$\begin{aligned} Q_{min} &= m_1+m_2+m_3+m_4, & Q_{max} &= M-m_5, \\ Q_{3,min} &= m_1+m_2+m_3, & Q_{3,max} &= Q-m_4, \\ Q_{2,min} &= m_1+m_2, & Q_{2,max} &= Q_3-m_3. \end{aligned} \quad (11)$$

Here $d\Omega_5 = d\cos\theta_5 d\pi_5$ is the solid angle element of the momentum of ν_τ in the rest frame of $\tau(P)$, $d\Omega_4 = d\cos\theta_4 d\pi_4$ is the solid angle element of $\vec{q}_4$ in the rest frame of $q_1^\mu+q_2^\mu+q_3^\mu+q_4^\mu$, $d\Omega_3 = d\cos\theta_3 d\pi_3$ is the solid angle element of $\vec{q}_3$ in the $q_1^\mu+q_2^\mu+q_3^\mu$ rest frame, and finally, $d\Omega_2 = d\cos\theta_2 d\pi_2$ is the solid angle element of $\vec{q}_2$ in the $q_1^\mu+q_2^\mu$ rest frame.

These formula if used directly, are inefficient for a Monte Carlo algorithm if sharp peaks due to resonances in the intermediate states are present. We refer to the `TAUOLA` documentation [11, 13] for details of the algorithm actually in use. For the present paper it is enough to note that those changes affect the program efficiency, but the actual density of the phase space remains intact. No approximations are introduced.

4 Hadronic current for 4π system

The model of Ref. [5] is based on the assumption that the $a_1(1260)\pi$ and $\omega\pi$ intermediate states (which well describe the experiments on $e^+e^- \to 4\pi$ [6]), are dominant in the amplitudes $\tau^+ \to \bar{\nu}_\tau \tilde{\rho}^+ \to \bar{\nu}_\tau (4\pi)^+$. In Ref. [5] it was shown that various two- and three-pion invariant mass distributions predicted by the model well describe experimental observations of CLEO [3] and ALEPH [20]. We include into consideration two most important channels of the $a_1 \to 3\pi$ decay ($a_1 \to \rho\pi \to 3\pi$ and $a_1 \to \sigma\pi \to 3\pi$) as well as the $\omega \to \rho\pi \to 3\pi$ channel. Then for the process $\tau^+ \to \bar{\nu}_\tau \pi^+\pi^0\pi^0\pi^0$ the current J^μ reads

$$J^\mu = J^\mu_{a_1\to\rho\pi} + J^\mu_{a_1\to\sigma\pi}. \quad (12)$$

For the process $\tau^+ \to \bar{\nu}_\tau \pi^+\pi^-\pi^+\pi^0$, where the ω meson also contributes, it is

$$J^\mu = J^\mu_{a_1\to\rho\pi} + J^\mu_{a_1\to\sigma\pi} + J^\mu_{\omega\to\rho\pi} \quad (13)$$

where in the following we neglect the interference between the ω and a_1 currents. The $\bar{\nu}_\tau\pi^+\pi^-\pi^+\pi^0$ final states produced with the two currents ($a_1(1260)\pi$ and $\omega\pi$) are effectively treated as distinct tau decay modes.

4.1 $\tau^+ \to \bar{\nu}_\tau \pi^+ \pi^0 \pi^0 \pi^0$ decay channel

For the $\tau^+ \to \bar{\nu}_\tau \pi^+(q_1)\pi^0(q_2)\pi^0(q_3)\pi^0(q_4)$ channel the current which includes possible Feynman diagrams [2], can be written in the following way:

$$J^\mu_{a_1\to\rho\pi} = G_{\pi^+\pi^0\pi^0\pi^0}(Q^2)[t_1^\mu(q_2,q_3,q_1,q_4) + t_1^\mu(q_2,q_4,q_1,q_3) + t_1^\mu(q_3,q_2,q_1,q_4) + t_1^\mu(q_3,q_4,q_1,q_2) + t_1^\mu(q_4,q_2,q_1,q_3) + t_1^\mu(q_4,q_3,q_1,q_2)], \quad (14)$$

$$J^\mu_{a_1\to\sigma\pi} = G_{\pi^+\pi^0\pi^0\pi^0}(Q^2)[t_2^\mu(q_2,q_1,q_3,q_4) + t_2^\mu(q_3,q_1,q_2,q_4) + t_2^\mu(q_4,q_1,q_3,q_2) - t_2^\mu(q_1,q_2,q_3,q_4) - t_2^\mu(q_1,q_3,q_2,q_4) - t_2^\mu(q_1,q_4,q_3,q_2)]. \quad (15)$$

Four-vectors t_1^μ and t_2^μ have the following forms, where Q denotes $Q = q_1 + q_2 + q_3 + q_4$:

$$t_1^\mu(q_1,q_2,q_3,q_4) = \frac{F_{a_1}^2(Q-q_1)}{D_{a_1}(Q-q_1)D_\rho(q_3+q_4)} \times \{Q\cdot(Q-q_1)[q_4^\mu(Q-q_1)\cdot q_3 - q_3^\mu(Q-q_1)\cdot q_4] + (Q^\mu - q_1^\mu)[(Q\cdot q_4)(q_1\cdot q_3) - (Q\cdot q_3)(q_4\cdot q_1)]\} \quad (16)$$

$$t_2^\mu(q_1,q_2,q_3,q_4) = \frac{zF_{a_1}^2(Q-q_1)}{D_{a_1}(Q-q_1)D_\sigma(q_3+q_4)} \times \{q_2^\mu Q\cdot(Q-q_1)(Q-q_1)^2 + (q_1^\mu - Q^\mu)[(Q\cdot q_2)(Q-q_1)^2]\}. \quad (17)$$

Here $1/D_{a_1}(q)$, $1/D_\rho(q)$ and $1/D_\sigma(q)$ are propagators of the a_1, ρ and σ mesons, $F_{a_1}(q)$ is the form factor and z is the dimensionless complex constant characterizing the relative fraction of the $\sigma\pi$ intermediate state in the $a_1(1260)$ decay. $G_{\pi^+\pi^0\pi^0\pi^0}$ is some function depending on Q^2 which we find by fitting the 4π invariant mass distribution [3]. As a F_{a_1} form factor, we used the function from [5,6], $F(q) = (1+m_{a_1}^2/\Lambda^2)/(1+q^2/\Lambda^2)$ with $\Lambda \sim 1$ GeV.

The form of the propagators is very important for analyzing the data. We represent the function $D(q)$ in the form used in [5, 6]

$$D(q) = q^2 - M^2 + iM\Gamma\frac{g(q^2)}{g(M^2)}, \quad (18)$$

where M and Γ are the mass and width of the corresponding particle, and the function $g(s)$ describes the dependence of the width on virtuality. In the case of the ρ meson the function $g_\rho(s)$ reads:

$$g_\rho(s) = s^{-1/2}(s-4m^2)^{3/2}, \quad (19)$$

while for the σ meson it is:

$$g_\sigma(s) = (s-4m^2/s)^{1/2}, \quad (20)$$

[2] Possible Feynman diagrams for τ^+ decays into 4π via the $a_1\pi$ and the $\omega\pi$ intermediate states are shown in Appendix A.

[3] For details see chapter **The $G(Q^2)$ functions**.

where m is the pion mass.

The function g_{a_1} in the a_1 propagator has the form:

$$g_{a_1}(s) = F^2_{a_1}(q) \int \Bigg\{ \left| \frac{\varepsilon_2 \mathbf{p}_1 - \varepsilon_1 \mathbf{p}_2}{D_\rho(p_1+p_2)} + \frac{\varepsilon_2 \mathbf{p}_3 - \varepsilon_3 \mathbf{p}_2}{D_\rho(p_2+p_3)} + \frac{z\sqrt{s}\mathbf{p}_2}{D_\sigma(p_1+p_3)} \right|^2$$

$$+ \frac{|z|^2 s}{3!} \left| \frac{\mathbf{p}_1}{D_\sigma(p_2+p_3)} + \frac{\mathbf{p}_2}{D_\sigma(p_1+p_3)} + \frac{\mathbf{p}_3}{D_\sigma(p_1+p_2)} \right|^2 \Bigg\} \times$$

$$\times \frac{d\mathbf{p}_1\, d\mathbf{p}_2\, d\mathbf{p}_3\ \delta^{(4)}(p_1+p_2+p_3-q)}{2\varepsilon_1 2\varepsilon_2 2\varepsilon_3 (2\pi)^5} \tag{21}$$

where $q^0 = \sqrt{s}$, $\mathbf{q} = 0$ and $p_i = (\varepsilon_i, \mathbf{p}_i)$ are the pion momenta in the rest frame of the $\tilde{\rho}$ (the center of mass frame of the 4π system). The first term corresponds to the $a_1 \to \pi^+\pi^-\pi^0$ decay while the second one to the $a_1 \to 3\pi^0$ decay.

4.2 $\tau^+ \to \bar{\nu}_\tau \pi^+\pi^-\pi^+\pi^0$ decay channel

For the $\tau^+ \to \bar{\nu}_\tau \pi^+(q_1)\pi^-(q_2)\pi^+(q_3)\pi^0(q_4)$ channel the current which includes the contribution from the ω meson intermediate state can be written in the following way:

$$J^\mu_{a_1\to\rho\pi} = G_{\pi^+\pi^-\pi^+\pi^0}(Q^2)[t_1^\mu(q_1,q_2,q_3,q_4) + t_1^\mu(q_3,q_2,q_1,q_4) + t_1^\mu(q_1,q_3,q_2,q_4)$$
$$+ t_1^\mu(q_3,q_1,q_2,q_4) + t_1^\mu(q_4,q_3,q_1,q_2) + t_1^\mu(q_4,q_1,q_3,q_2)], \tag{22}$$

$$J^\mu_{a_1\to\sigma\pi} = G_{\pi^+\pi^-\pi^+\pi^0}(Q^2)[t_2^\mu(q_4,q_3,q_1,q_2) + t_2^\mu(q_4,q_1,q_3,q_2)$$
$$- t_2^\mu(q_1,q_4,q_3,q_2) - t_2^\mu(q_3,q_4,q_1,q_2)], \tag{23}$$

$$J^\mu_{\omega\to\rho\pi} = G^\omega_{\pi^+\pi^-\pi^+\pi^0}(Q^2)[t_3^\mu(q_1,q_2,q_3,q_4) + t_3^\mu(q_3,q_2,q_1,q_4) - t_3^\mu(q_1,q_3,q_2,q_4)$$
$$- t_3^\mu(q_3,q_1,q_2,q_4) - t_3^\mu(q_1,q_4,q_3,q_2) - t_3^\mu(q_3,q_4,q_1,q_2)]. \tag{24}$$

Here four-vectors t_1^μ, t_2^μ are the same as in the previous case and t_3^μ reads:

$$t_3^\mu(q_1,q_2,q_3,q_4) = \frac{F^2_\omega(Q-q_1)}{D_\omega(Q-q_1)D_\rho(q_3+q_4)} \qquad \times$$

$$\{q_2^\mu[(Q\cdot q_3)(q_1\cdot q_4) - (Q\cdot q_4)(q_1\cdot q_3)] - Q\cdot q_2[q_3^\mu(q_1\cdot q_4) - q_4^\mu(q_1\cdot q_3)]$$
$$+ (q_1\cdot q_2)[q_3^\mu(Q\cdot q_4) - q_4^\mu(Q\cdot q_3)]\}, \tag{25}$$

where $F_\omega(q)$ and $D_\omega(q)$ are the form factor and propagator for the ω. Because of the small width of the ω we set $F_\omega(q) = 1$ and $g_\omega(s) = 1$. $G_{\pi^+\pi^-\pi^+\pi^0}$ and $G^\omega_{\pi^+\pi^-\pi^+\pi^0}$ are functions of Q^2.

Table 1: *The masses and widths for the intermediate states.*

Intermediate state	Mass, GeV	Width, GeV
$\rho(770)$	0.7761	0.1445
$a_1(1260)$	1.23	0.45
$\omega(782)$	0.782	0.00841
σ	0.8	0.8

5 Parameters used in the model

The constants, widths and other parameters used in our numerical results were mainly taken from [21], for the ρ meson recent CMD-2 results were used [22]. Some of them are collected in Table 1, The $m_\nu = 0$ was assumed and `PHOTOS` [23, 24] for QED radiative corrections was switched off. We used a τ lepton mass of m_τ=1.777 GeV and the physical masses for the pions in the phase space, *i.e.* $m_{\pi^\pm} = 0.13957018$ GeV, $m_{\pi^0} = 0.1349766$ GeV. Note that because of CVC the masses of $\pi^\pm$ and π^0 were set equal $m_{\pi^0} = m_{\pi^\pm} = 0.139570$ in the hadronic current. The parameter $\Lambda = 1.2$ GeV for the F_{a_1} form factor was taken. The dimensionless complex constant z for $t_2^\mu(q_1, q_2, q_3, q_4)$ and for $g_{a_1}(s)$ was set to $(1.269, 0.591)$ which means that the ratio of contributions of the σ to ρ intermediate states is 0.3 accordingly to Ref. [26].

5.1 The $G(Q^2)$ functions

New channels in `TAUOLA` are based on the same matrix elements for the $\tilde{\rho}^+$ decay as in [5]. The difference is in Q^2 generation. To complete the definition of the hadronic current, the appropriate choice of the three functions $G(Q^2)$ was needed. We fit the functions $G_{\pi^+\pi^0\pi^0\pi^0}(Q^2)$, $G_{\pi^+\pi^-\pi^+\pi^0}(Q^2)$, and $G^{\omega}_{\pi^+\pi^-\pi^+\pi^0}(Q^2)$ in such a way, that `TAUOLA` reproduces predictions from the calculation [5] for the single variable $d\Gamma/dQ^2$ distribution. Samples of 5 000 000 events were used. The table of numerical values for the fitted functions is given in Appendix B. The functions are well determined by the e^+e^- data from 0.9 to 1.7 GeV, for lower energies the uncertainties are larger since the measured cross section is small, and we rely on assumptions made in Ref. [5].

Finally, we have normalized the functions $G(Q^2)$ in such a way that our program reproduces τ decay rates of Ref. [21], see results in Table 2.

Table 2: *Numerical results for the integrated decay rates of our model*

Channel	Decay rate, GeV
$\Gamma(\tau^+ \to \bar{\nu}_\tau \pi^0 \pi^0 \pi^0 \pi^+)$	$2.4462 * 10^{-14}$
$\Gamma(\tau^+ \to \bar{\nu}_\tau \pi^+ \pi^+ \pi^- \pi^0)$	$9.5130 * 10^{-14}$

6 Numerical tests

6.1 Technical test

While developing the Monte Carlo algorithm, it is important to perform numerous technical tests of the Monte Carlo code. Tests of the TAUOLA Monte Carlo library consisting of the comparison of numerical results obtained from the program and independent semi-analytical calculations are described and listed in Ref. [13]. At that time the agreement between the Monte Carlo results and some analytical calculations was pushed to the level of few permille. Recently, thanks to much faster computers, checks at the 0.1 % level were in some cases redone. In those tests different assumptions about matrix elements were used, *e.g.* masses of $\pi^\pm$ and π^0 were set equal or even zero. The actual choice of the current was also modified. Parameters of the presamples were varied and results were checked to be independent of that. Satisfactory agreement was always found. This gives us confidence in the technical side of the algorithm.

6.2 General test

We have compared various possible invariant mass distributions constructed from the momenta of the τ decay products in the Novosibirsk model coded in TAUOLA on one side to the code used in Ref. [5] on the other side. The samples used in the plots were of the size of the experimental data used as an input to the model, *i.e.* 30 000 events. In each case agreement was sufficiently good, for details see [25]. In this way we could convince ourselves that the adaptation was really correct.

7 Comparison with other parameterizations

Once we became confident in the correct implementation of the new Novosibirsk model, we have decided to compare its predictions to another one. For that purpose we have chosen the model tuned to the 1998 CLEO data because it is still quite often used.

In this section we collect predictions for all possible invariant mass distributions for the decay channels: $\tau \to \bar{\nu}_\tau \pi^+ \pi^- \pi^+ \pi^0$ and $\tau \to \bar{\nu}_\tau \pi^+ \pi^0 \pi^0 \pi^0$. In Figs. 1 to 7 we compare predictions of our new Novosibirsk current with the older CLEO current [1, 17–19], both

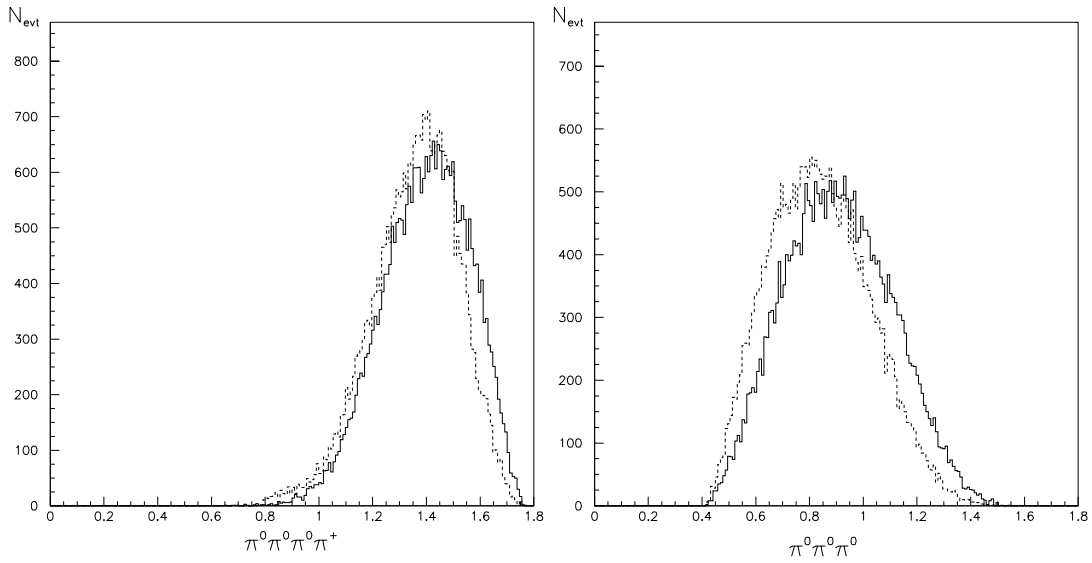

Figure 1: *The $\bar{\nu}_\tau\pi^0\pi^0\pi^0\pi^+$ channel. The left-hand side plots the $\pi^0\pi^0\pi^0\pi^+$ invariant mass distribution and the right-hand side is the $\pi^0\pi^0\pi^0$ invariant mass distribution. The continuous and dotted lines correspond to the old CLEO and new Novosibirsk current respectively.*

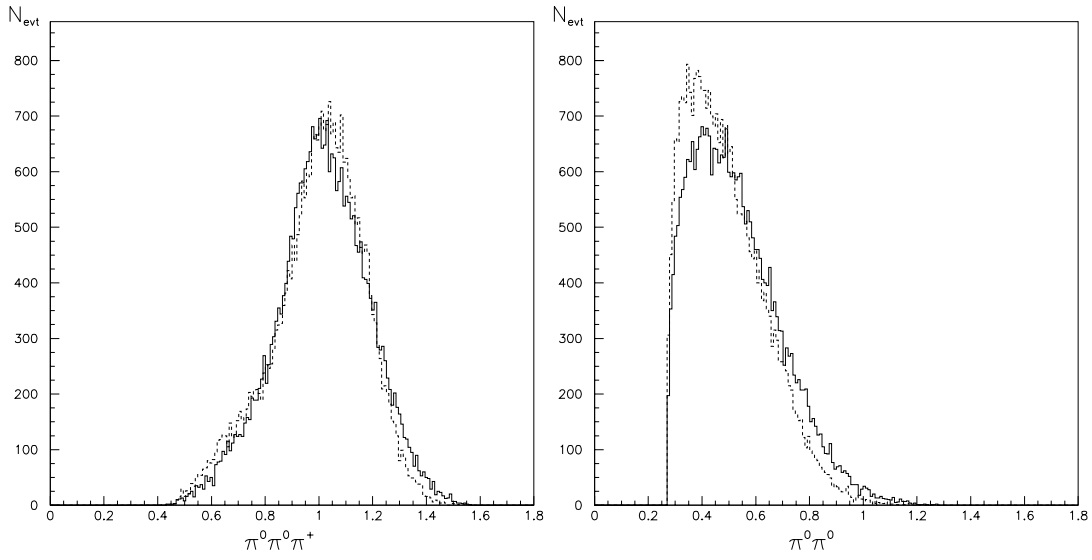

Figure 2: *The $\bar{\nu}_\tau\pi^0\pi^0\pi^0\pi^+$ channel. The left-hand side plots the $\pi^0\pi^0\pi^+$ invariant mass distribution and the right-hand side is the $\pi^0\pi^0$ invariant mass distribution. The continuous and dotted lines correspond to the old CLEO and new Novosibirsk current respectively.*

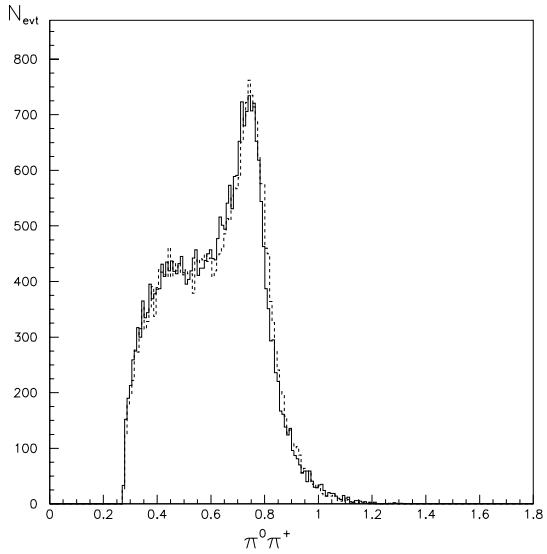

Figure 3: *The $\pi^0\pi^+$ invariant mass distribution for the $\bar{\nu}_\tau\pi^0\pi^0\pi^0\pi^+$ channel. The continuous and dotted lines correspond to the old CLEO and new Novosibirsk current respectively.*

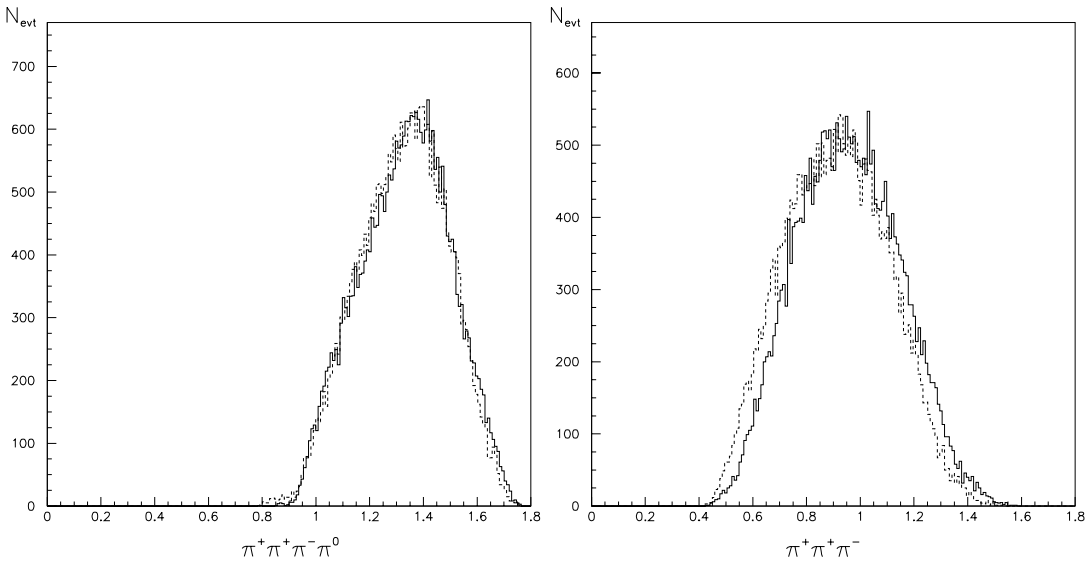

Figure 4: *The $\bar{\nu}_\tau\pi^+\pi^+\pi^-\pi^0$ channel. The left-hand side plots the $\pi^+\pi^+\pi^-\pi^0$ invariant mass distribution and the right-hand side is the $\pi^+\pi^+\pi^-$ invariant mass distribution. The continuous and dotted lines correspond to the old CLEO and new Novosibirsk current respectively.*

implemented in the `TAUOLA` Monte Carlo library as options:

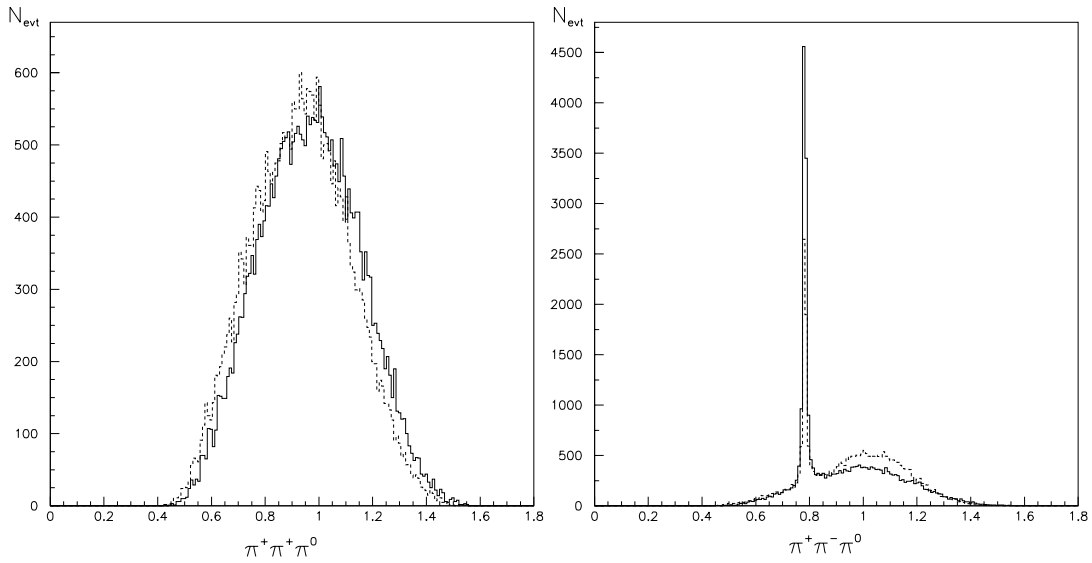

Figure 5: *The $\bar{\nu}_\tau\pi^+\pi^+\pi^-\pi^0$ channel. The left-hand side plots the $\pi^+\pi^+\pi^0$ invariant mass distribution and the right-hand side is the $\pi^+\pi^-\pi^0$ invariant mass distribution. The continuous and dotted lines correspond to the old CLEO and new Novosibirsk current respectively.*

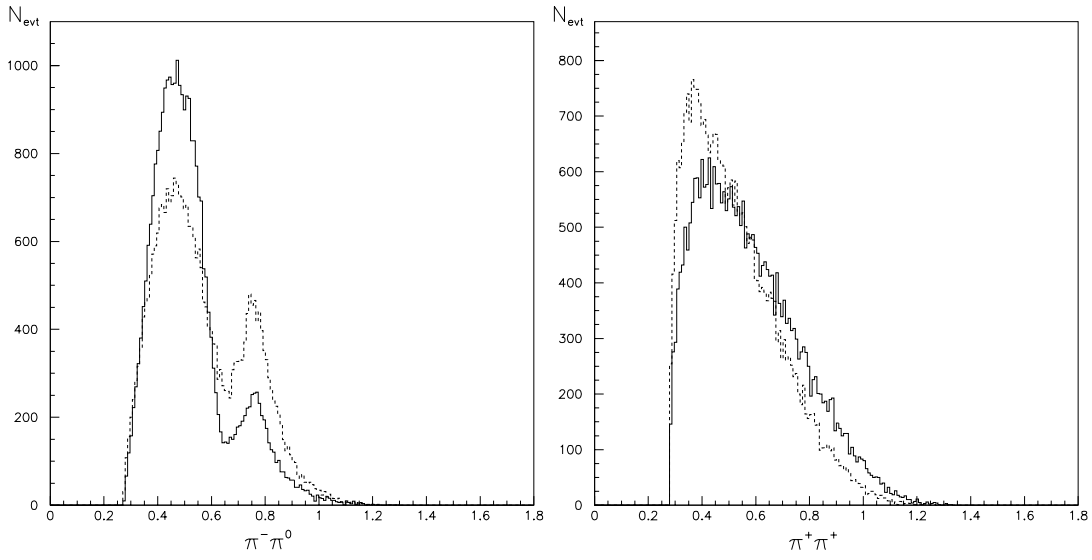

Figure 6: *The $\bar{\nu}_\tau\pi^+\pi^+\pi^-\pi^0$ channel. The left-hand side plots the $\pi^-\pi^0$ invariant mass distribution and the right-hand side is the $\pi^+\pi^+$ invariant mass distribution. The continuous and dotted lines correspond to the old CLEO and new Novosibirsk current respectivevly.*

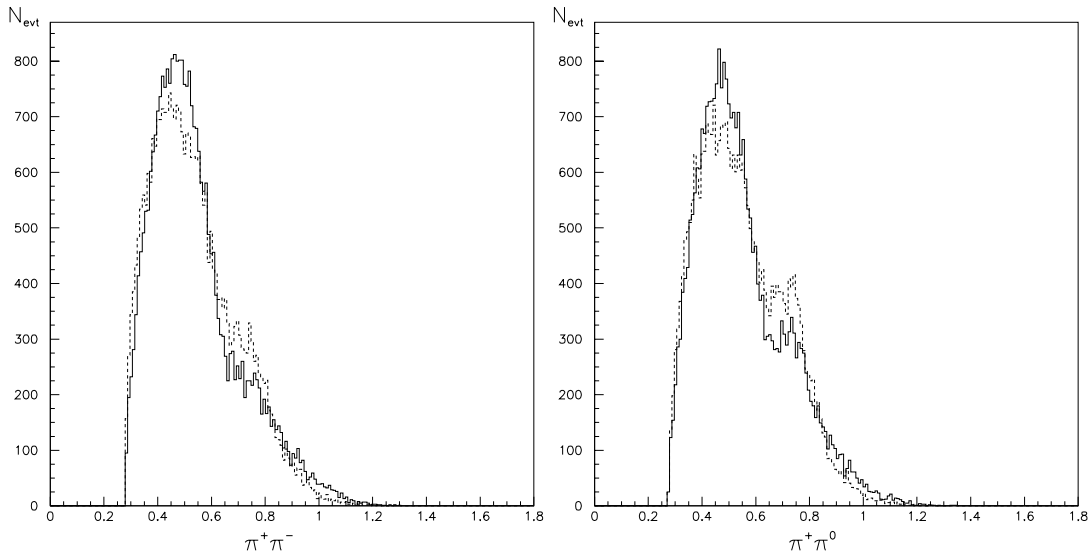

Figure 7: *The $\bar{\nu}_\tau\pi^+\pi^+\pi^-\pi^0$ channel. The left-hand side plots the $\pi^+\pi^-$ invariant mass distribution and the right-hand side is the $\pi^+\pi^0$ invariant mass distribution. The continuous and dotted lines correspond to the old CLEO and new Novosibirsk current respectively.*

- $\tau^+ \to \bar{\nu}_\tau\pi^+\pi^0\pi^0\pi^0$ channel

In the first part of this chapter the invariant mass distributions for $\tau^+ \to \bar{\nu}_\tau\pi^+\pi^0\pi^0\pi^0$ channel are shown. In Fig. 1 we show the invariant mass distribution for $\pi^0\pi^0\pi^0\pi^+$ (left-hand side plot) and $\pi^0\pi^0\pi^0$ (right-hand side plot) systems. In Fig. 2 we show the invariant mass distribution for $\pi^0\pi^0\pi^+$ (left-hand side plot) and $\pi^0\pi^0$ (right-hand side plot) systems, and in Fig. 3 the invariant mass distribution for $\pi^0\pi^+$ system. In all plots the continuous and dotted lines correspond to the old (1998) CLEO and new Novosibirsk current.

- $\tau^+ \to \bar{\nu}_\tau\pi^+\pi^-\pi^+\pi^0$ channel

In the second part of this chapter the invariant mass distributions for $\tau^+ \to \bar{\nu}_\tau\pi^+\pi^-\pi^+\pi^0$ channel are shown. In Fig. 4 we show the invariant mass distribution for $\pi^+\pi^+\pi^-\pi^0$ (left-hand side plot) and $\pi^+\pi^+\pi^-$ (right-hand side plot) systems. In Fig. 5 we show the invariant mass distribution for $\pi^+\pi^+\pi^0$ (left-hand side plot) and $\pi^+\pi^-\pi^0$ (right-hand side plot) systems. In Fig. 6 we show the invariant mass distribution for $\pi^+\pi^0$ (left-hand side plot) and $\pi^+\pi^+$ (right-hand side plot) systems. In Fig. 7 we show the invariant mass distribution for $\pi^+\pi^-$ (left-hand side plot) and $\pi^+\pi^0$ (right-hand side plot) systems.

In some cases agreement is only qualitatively correct, but one should have in mind rather limited data samples available at that time[4]. We expect the Novosibirsk model to

[4]The largest differences are present in the $\tau^+ \to \bar{\nu}_\tau\pi^+\pi^-\pi^+\pi^0$ decay channel. They can be substantially diminished, if the $\omega\pi$ contribution to the current used in the CLEO model is appropriately

represent a substantial improvement over the old one.

8 Summary

The new parameterization of 4π form factors for the `TAUOLA` package is now available. The form factors are completely defined from the information in the paper. The particular strength of the model used in their definition relies on its success in describing high statistics low energy e^+e^- data at $\sqrt{s} < 1.4$ GeV (future experiments at the upgraded collider VEPP-2000 will extend the energy range to the τ lepton mass [27]). The CVC hypothesis has been instrumental in constructing predictions for the τ decays. The correctness of the code was checked by its comparison to the other generator based on the same data. Results obtained from our new form factors can be now used for comparisons with other models and τ lepton decay data directly under conditions of any present or future experiment.

Acknowledgements

Two of the authors (T.P. and M.W.) are very grateful for the warm hospitality extended to them by the Budker Institute of Nuclear Physics in Novosibirsk, where the sizable part of this work was performed.

reduced [25] to match the present measurements.

Appendix A

Feynman diagrams for τ^+ decays into 4π

Taking into account the quantum numbers of all intermediate and final states, see Table 3, the following Feynman diagrams can be written for the τ^+ decay into $\bar{\nu}_\tau\pi^+\pi^0\pi^0\pi^0$ and $\bar{\nu}_\tau\pi^+\pi^-\pi^+\pi^0$, if $a_1(1260)\pi$ and $\omega\pi$ intermediate states are assumed.

Table 3: *The quantum numbers of mesons.*

Intermediate state	I^G	J^{PC}
$\rho(770)$ $(\tilde{\rho})$	1^+	1^{--}
$\pi^\pm$	1^-	0^-
π^0	1^-	0^{-+}
$a_1(1260)$	1^-	1^{++}
$\omega(782)$	0^-	1^{--}
σ	0^+	0^{++}

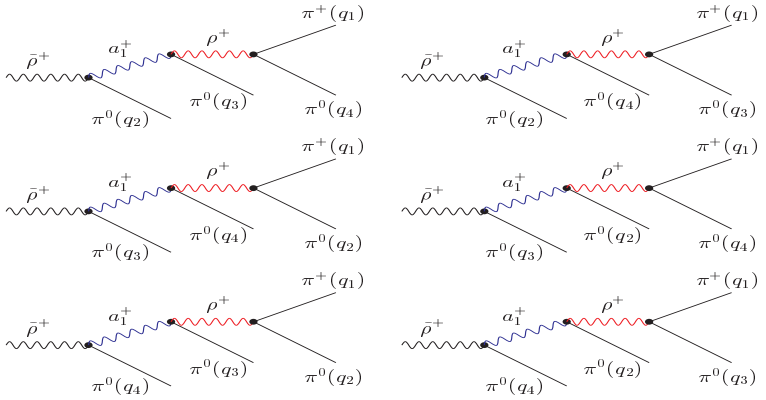

Figure 8: *Diagrams for the $\tau^+ \to \bar{\nu}_\tau\pi^+(q_1)\pi^0(q_2)\pi^0(q_3)\pi^0(q_4)$ decay via the $\tilde{\rho}^+ \to a_1\pi \to \rho\pi\pi \to \pi\pi\pi\pi$ intermediate states.*

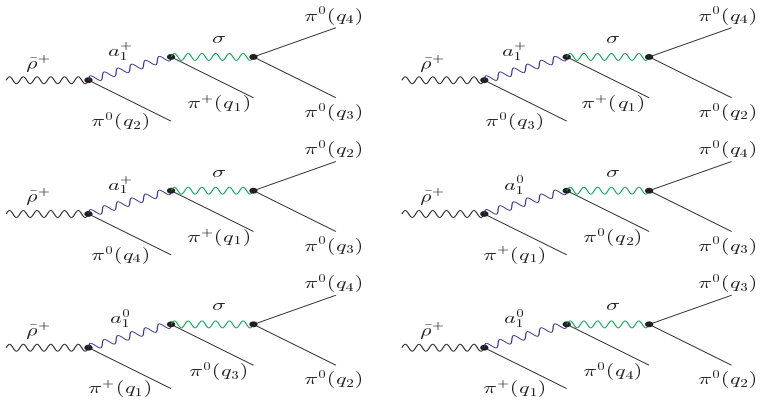

Figure 9: *Diagrams for the* $\tau^+ \to \bar{\nu}_\tau \pi^+(q_1)\pi^0(q_2)\pi^0(q_3)\pi^0(q_4)$ *decay channel via the* $\tilde{\rho}^+ \to a_1\pi \to \sigma\pi\pi \to \pi\pi\pi\pi$ *intermediate states.*

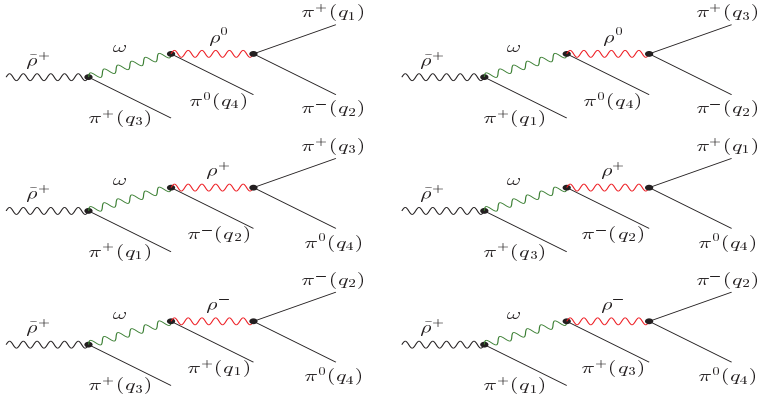

Figure 10: *Diagrams for the* $\tau^+ \to \bar{\nu}_\tau \pi^+(q_1)\pi^-(q_2)\pi^+(q_3)\pi^0(q_4)$ *decay via the* $\tilde{\rho}^+ \to \omega\pi \to \rho\pi\pi \to \pi\pi\pi\pi$ *intermediate states.*

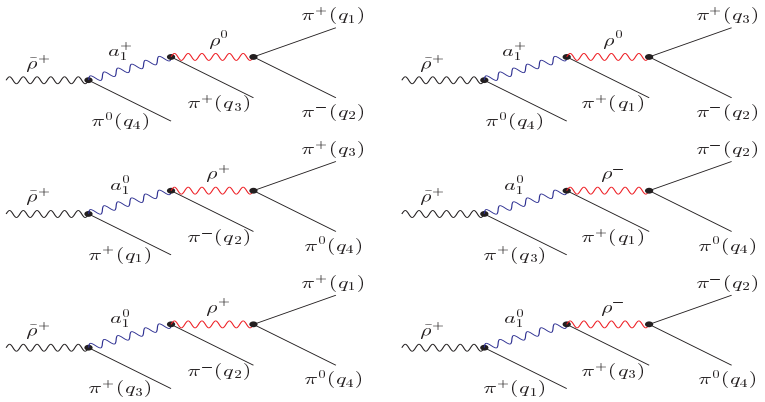

Figure 11: *Diagrams for the* $\tau^+ \to \bar{\nu}_\tau \pi^+(q_1)\pi^-(q_2)\pi^+(q_3)\pi^0(q_4)$ *decay via the* $\tilde{\rho}^+ \to a_1\pi \to \rho\pi\pi \to \pi\pi\pi\pi$ *intermediate states.*

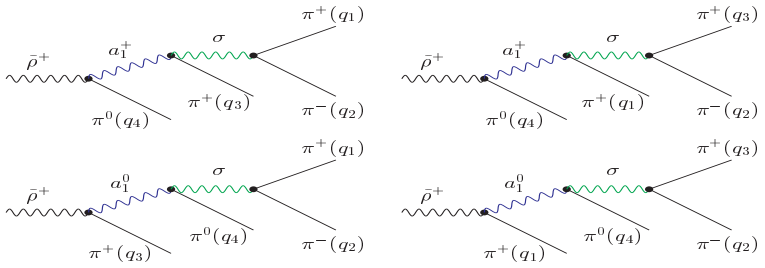

Figure 12: *Diagrams for the* $\tau^+ \to \bar{\nu}_\tau \pi^+(q_1)\pi^-(q_2)\pi^+(q_3)\pi^0(q_4)$ *decay via the* $\tilde{\rho}^+ \to a_1\pi \to \sigma\pi\pi \to \pi\pi\pi\pi$ *intermediate states*

Appendix B

Tables of numerical values for functions $G(Q^2)$

Tables of numerical values for the $G_{\pi^+\pi^0\pi^0\pi^0}(Q^2)$, $G_{\pi^+\pi^-\pi^+\pi^0}(Q^2)$, and $G^{\omega}_{\pi^+\pi^-\pi^+\pi^0}(Q^2)$ functions at 96 energy points are given. In Table 4.A the $G_{\pi^+\pi^0\pi^0\pi^0}(Q^2)$ function for the $\pi^+\pi^0\pi^0\pi^0$ decay channel - part of the current dominated by the $a_1\pi$ intermediate state is given. In Table 4.B the $G_{\pi^+\pi^-\pi^+\pi^0}(Q^2)$ function for the $\pi^+\pi^-\pi^+\pi^0$ decay channel - part of the current dominated by the $a_1\pi$ intermediate state is given , and finally in Table 4.C the $G^{\omega}_{\pi^+\pi^-\pi^+\pi^0}(Q^2)$ for the $\pi^+\pi^-\pi^+\pi^0$ decay channel - and $\omega\pi$ intermediate state.

A $G_{\pi^+\pi^0\pi^0\pi^0}(Q^2)$

Q^2	$G(Q^2)$	Q^2	$G(Q^2)$	Q^2	$G(Q^2)$
0.600	0.000	1.033	1.328	1.467	0.932
0.613	0.000	1.046	1.317	1.480	0.928
0.626	0.000	1.060	1.304	1.493	0.924
0.639	0.000	1.073	1.297	1.506	0.924
0.653	0.000	1.086	1.280	1.519	0.917
0.666	0.000	1.099	1.265	1.532	0.918
0.679	0.000	1.112	1.256	1.545	0.912
0.692	0.000	1.125	1.233	1.559	0.905
0.705	0.000	1.138	1.221	1.572	0.907
0.718	0.000	1.152	1.194	1.585	0.903
0.731	0.000	1.165	1.175	1.598	0.899
0.744	0.000	1.178	1.151	1.611	0.901
0.758	0.000	1.191	1.136	1.624	0.904
0.771	0.000	1.204	1.121	1.637	0.895
0.784	0.000	1.217	1.101	1.651	0.890
0.797	1.482	1.230	1.090	1.664	0.891
0.810	1.709	1.243	1.073	1.677	0.885
0.823	1.696	1.257	1.058	1.690	0.889
0.836	1.617	1.270	1.044	1.703	0.887
0.849	1.630	1.283	1.038	1.716	0.900
0.863	1.572	1.296	1.025	1.729	0.898
0.876	1.546	1.309	1.010	1.742	0.910
0.889	1.538	1.322	1.004	1.756	0.905
0.902	1.501	1.335	0.994	1.769	1.745
0.915	1.492	1.348	0.986	1.782	0.000
0.928	1.472	1.362	0.977	1.795	0.000
0.941	1.437	1.375	0.972	1.808	0.000
0.955	1.399	1.388	0.966	1.821	0.000
0.968	1.388	1.401	0.961	1.834	0.000
0.981	1.403	1.414	0.953	1.847	0.000
0.994	1.377	1.427	0.949	1.861	0.000
1.007	1.349	1.440	0.942	1.874	0.000

B $G_{\pi^+\pi^-\pi^+\pi^0}(Q^2)$

Q^2	$G(Q^2)$	Q^2	$G(Q^2)$	Q^2	$G(Q^2)$
0.600	0.000	1.033	2.689	1.467	0.932
0.613	0.000	1.046	2.520	1.480	0.912
0.626	0.000	1.060	2.468	1.493	0.892
0.639	0.000	1.073	2.354	1.506	0.872
0.653	0.000	1.086	2.212	1.519	0.852
0.666	0.000	1.099	2.110	1.532	0.828
0.679	0.000	1.112	2.011	1.545	0.806
0.692	0.000	1.125	1.879	1.559	0.777
0.705	0.000	1.138	1.825	1.572	0.757
0.718	0.000	1.152	1.707	1.585	0.738
0.731	0.000	1.165	1.644	1.598	0.710
0.744	0.000	1.178	1.550	1.611	0.685
0.758	0.000	1.191	1.481	1.624	0.667
0.771	0.000	1.204	1.423	1.637	0.637
0.784	0.000	1.217	1.363	1.651	0.616
0.797	13.166	1.230	1.321	1.664	0.601
0.810	10.723	1.243	1.278	1.677	0.580
0.823	8.822	1.257	1.239	1.690	0.567
0.836	10.799	1.270	1.198	1.703	0.545
0.849	9.188	1.283	1.163	1.716	0.535
0.863	7.853	1.296	1.132	1.729	0.513
0.876	7.748	1.309	1.111	1.742	0.493
0.889	8.263	1.322	1.095	1.756	0.531
0.902	5.504	1.335	1.069	1.769	0.857
0.915	4.903	1.348	1.060	1.782	0.000
0.928	4.479	1.362	1.039	1.795	0.000
0.941	3.965	1.375	1.022	1.808	0.000
0.955	4.525	1.388	1.015	1.821	0.000
0.968	3.651	1.401	1.001	1.834	0.000
0.981	3.501	1.414	0.991	1.847	0.000
0.994	3.227	1.427	0.971	1.861	0.000
1.007	3.181	1.440	0.960	1.874	0.000

C $G^{\omega}_{\pi^+\pi^-\pi^+\pi^0}(Q^2)$

Q^2	$G(Q^2)$	Q^2	$G(Q^2)$	Q^2	$G(Q^2)$
0.600	0.000	1.033	1.927	1.467	0.720
0.613	0.000	1.046	1.867	1.480	0.689
0.626	0.000	1.060	1.791	1.493	0.657
0.639	0.000	1.073	1.718	1.506	0.626
0.653	0.000	1.086	1.654	1.519	0.594
0.666	0.000	1.099	1.604	1.532	0.566
0.679	0.000	1.112	1.554	1.545	0.539
0.692	0.000	1.125	1.507	1.559	0.510
0.705	0.000	1.138	1.461	1.572	0.479
0.718	0.000	1.152	1.422	1.585	0.455
0.731	0.000	1.165	1.385	1.598	0.432
0.744	0.000	1.178	1.348	1.611	0.406
0.758	0.000	1.191	1.315	1.624	0.377
0.771	0.000	1.204	1.279	1.637	0.356
0.784	0.000	1.217	1.249	1.651	0.333
0.797	0.000	1.230	1.218	1.664	0.314
0.810	0.000	1.243	1.195	1.677	0.295
0.823	0.000	1.257	1.168	1.690	0.281
0.836	0.000	1.270	1.146	1.703	0.260
0.849	0.000	1.283	1.115	1.716	0.235
0.863	0.000	1.296	1.094	1.729	0.227
0.876	0.000	1.309	1.061	1.742	0.219
0.889	0.000	1.322	1.039	1.756	0.229
0.902	0.000	1.335	1.016	1.769	0.284
0.915	2.287	1.348	0.991	1.782	0.000
0.928	2.971	1.362	0.959	1.795	0.000
0.941	2.934	1.375	0.931	1.808	0.000
0.955	2.691	1.388	0.902	1.821	0.000
0.968	2.547	1.401	0.873	1.834	0.000
0.981	2.356	1.414	0.845	1.847	0.000
0.994	2.245	1.427	0.815	1.861	0.000
1.007	2.107	1.440	0.782	1.874	0.000

Table 4: *The tables of numerical values for the following functions:*
(A) $G_{\pi^+\pi^0\pi^0\pi^0}(Q^2)$ *used in the* $\pi^+\pi^0\pi^0\pi^0$ *decay channel and* $a_1\pi$ *intermediate state.*
(B) $G_{\pi^+\pi^-\pi^+\pi^0}(Q^2)$ *used in the* $\pi^+\pi^-\pi^+\pi^0$ *decay channel and* $a_1\pi$ *intermediate state.*
(C) $G^{\omega}_{\pi^+\pi^-\pi^+\pi^0}(Q^2)$ *used in the* $\pi^+\pi^-\pi^+\pi^0$ *decay channel and* $\omega\pi$ *intermediate state.*

References

[1] R. Decker, M. Finkemeier, P. Heiliger, H. H. Jonson, *Z. Phys.* **C70**, 247 (1996).

[2] H. Czyż, J. H. Kühn, *Eur. Phys. J.* **C18**, 497 (2001).

[3] K. W. Edwards *et al.*, [CLEO Collaboration], *Phys. Rev.* **D61**, 072003 (2000).

[4] A. J. Weinstein, [CLEO Collaboration], *Nucl. Phys. (Proc. Suppl.)*, **98**, 261 (2001), and references therein.

[5] A. E. Bondar, S. I. Eidelman, A. I. Milstein, N. I. Root, *Phys. Lett.* **B466**, 403 (1999).

[6] R. R. Akhmetshin *et al.*, [CMD-2 Collaboration], *Phys. Lett.* **B466**, 392 (1999).

[7] Y. S. Tsai, *Phys. Rev.* **D4**, 2821 (1971).

[8] S. I. Eidelman and V. N. Ivanchenko, *Nucl. Phys. B (Proc. Suppl.)* **76**, 319 (1999).

[9] R. R Akhmetshin *et al.*, [CMD-2 Collaboration], Preprint Budker INP 95-62, Novosibirsk, 1995.

[10] M. N. Achasov *et al.*, [SND Collaboration], Preprint Budker INP 98-65, Novosibirsk, 1998.

[11] S. Jadach, J. H. Kühn and Z. Wąs, *Comput. Phys. Commun.* **64**, 275 (1990).

[12] S. Jadach, M. Jeżabek, J. H. Kühn and Z. Wąs, *Comput. Phys. Commun.* **70**, 69 (1992).

[13] R. Decker, S. Jadach, J. H. Kühn and Z. Wąs, *Comput. Phys. Commun.* **76**, 361 (1993).

[14] P. Golonka, E. Richter-Wąs and Z. Wąs, `hep-ph/0009302.`

[15] T. Pierzchała, E. Richter-Wąs, Z. Wąs and M. Worek, *Acta Phys. Polon.* **B32**, 1277 (2001).

[16] A. J. Weinstein, [CLEO Collaboration], see www home page:
`http://www.cithep.caltech.edu/~ajw/korb_doc.html#files`.

[17] R. Fisher, J. Wess and F. Wagner, *Z. Phys.* **C3**, 313 (1979).

[18] R. Decker, *Z. Phys.* **C36**, 487 (1987).

[19] M. Gell-Mann, D. Sharp, W. Wagner, *Phys. Rev. Lett.* **8**, 261 (1962).

[20] D. Busculic *et al.*, [ALEPH Collaboration], *Z. Phys.* **C74**, 263 (1997).

[21] D. E. Groom *et al.*, [Particle Date Group Collaboration], *Eur. Phys. J.* **C15**, 1 (2000).

[22] R. R. Akhmetshin *et al.*, [CMD-2 Collaboration], accepted for publication in *Phys. Lett.* **B**, hep-ex/0112031.

[23] E. Barberio, B. van Eijk, Z. Wąs, *Comput. Phys. Commun.* **66**, 115 (1991).

[24] E. Barberio, Z. Wąs, *Comput. Phys. Commun.* **79**, 291 (1994).

[25] For the additional appendices to the present paper see:
http://lhotse.ifj.edu.pl/~pierzchala/4pi-Novosibirsk.html,
or http://www.cern.ch/~wasm.

[26] D. Asner *et al.*, [CLEO Collaboration], *Phys. Rev.* **D61**, 012002 (2000).

[27] Yu. M. Shatunov *et al.*, *Proceedings of the EPAC 2000*, Vienna, Austria, p.439.